

Measurements of the Diffractive Structure Function $F_2^{D(3)}(\beta, Q^2, x_P)$ at HERA.

Paul Newman^{*†} (for the H1 and ZEUS Collaborations)

School of Physics and Astronomy, University of Birmingham, B15 2TT, UK.

E-mail: prn@hep.ph.bham.ac.uk

ABSTRACT: Recent measurements of the diffractive cross section in deep-inelastic scattering (DIS) at HERA are presented. The data are used to investigate the factorisation properties of diffractive DIS and to examine its quantum chromodynamic (QCD) structure. Models based on the colour dipole approach to DIS are also tested.

1. Diffractive Deep Inelastic Scattering

At low x in DIS at HERA, approximately 10% of the events are of the type $ep \rightarrow eXp$, where the final state proton carries in excess of 95% of the proton beam energy [1, 2]. The kinematics of these processes are illustrated in figure 1. A photon of virtuality Q^2 , coupled to the electron, undergoes a strong interaction with the proton to form a final state hadronic system X (mass M_X) separated by a large rapidity gap from the leading proton. No net quantum numbers are exchanged. A fraction x_P of the proton longitudinal momentum is transferred to the system X . The virtual photon couples to a quark carrying a fraction β of the exchanged momentum. The squared four-momentum transfer at the proton vertex is denoted t .

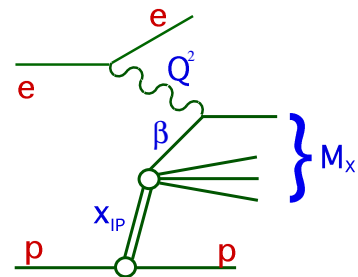


Figure 1: Illustration of the kinematic variables used to describe diffractive DIS.

Events with this ‘diffractive’ topology are interpreted in Regge models in terms of pomeron trajectory exchange between the proton and the virtual photon. The large photon virtualities encourage a perturbative QCD treatment of the process. However, the parton level interpretation is not obvious. In order to generate an exchange with net vacuum quantum numbers, a minimum of two partons must be exchanged in the t channel.

The differential cross section for diffractive DIS is often presented in terms of a diffractive structure function $F_2^{D(4)}(\beta, Q^2, x_P, t)$, defined analogously to the inclusive proton structure function F_2 . Experimentally, two complementary methods have been used to

^{*}Speaker.

[†]Supported by the UK Particle Physics and Astronomy Research Council (PPARC).

measure F_2^D . Recent measurements in which the leading proton is measured in proton spectrometers are described in [3]. In this contribution, data are presented for which it is not required that the leading proton is detected and the kinematics are reconstructed from the hadronic system X . This latter method yields the better statistical precision, but does not allow a measurement of t . The results are therefore presented in the form of a structure function $F_2^{D(3)}(\beta, Q^2, x_p)$, corresponding to an integral of $F_2^{D(4)}$ over t .

The H1 collaboration recently released new preliminary $F_2^{D(3)}$ data [4] (see figures 2 and 3) based on a factor of 5 more luminosity than previous measurements.¹ In the following sections, these data are used together with previous data from ZEUS and H1 to test the factorisation properties of diffractive DIS and its relationship to inclusive DIS.

2. Factorisation Properties and Diffractive Parton Densities

In [4], the β and Q^2 dependence of $F_2^{D(3)}$ is studied with high precision by measuring the structure function at four fixed values of $x_p = 0.001, 0.003, 0.01$ and 0.03 . As examples, the results for $x_p = 0.003$ are shown in figures 2 and 3. In figure 2, scaling violations with positive $\partial F_2^D / \partial \ln Q^2$ persist up to large values of $\beta > 0.4$, confirming earlier results [1, 2]. Since $x = \beta \cdot x_p$, the scaling violations in figure 2 can be compared with the scaling violations of the inclusive F_2 at the same value of x . When compared at fixed x , the Q^2 dependences of F_2 and F_2^D are similar for $\beta \lesssim 0.65$ in the diffractive case, suggesting that similar dynamics are at work in the two processes. At the highest β , the logarithmic Q^2 derivative of F_2^D becomes negative and there is a clear difference between the inclusive and diffractive Q^2 dependences at the same x [4]. In this high β region, higher twist contributions such as elastic vector meson production are thought to play a major role in the diffractive cross section [5]. The β dependence of F_2^D (figure 3) is relatively flat.

In [6], hard scattering factorisation was proven for a general class of semi-inclusive processes in DIS. A particular case is leading proton production with specified values of x_p and t , corresponding to the final states measured in diffractive DIS at HERA. The x and Q^2 dependence of the leading twist component of diffractive DIS can thus be treated in an analogous way to inclusive DIS. ‘Diffractive parton densities’ of the proton can be defined, which evolve according to the DGLAP equations and can be used to calculate observable cross sections when combined with suitable coefficient functions.

¹The new H1 data are integrated over $|t| < 1 \text{ GeV}^2$ and include a small contribution (5 – 10%) from processes in which the proton dissociates to a system of mass less than 1.6 GeV.

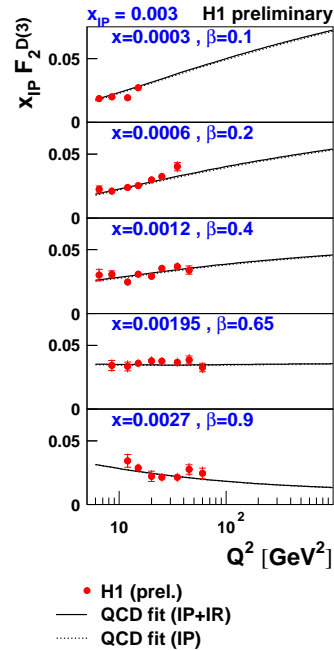


Figure 2: Dependence of $x_p F_2^D$ on Q^2 for different β values, with fixed $x_p = 0.003$. The data are compared with the DGLAP QCD fit described in the text (from [4]).

In figures 2 and 3, the data are compared with the results of a fit in which the (β, Q^2) dependence is obtained by parameterising the diffractive light quark and gluon densities at $Q_0^2 = 2 \text{ GeV}^2$ and evolving to higher Q^2 using the leading order DGLAP equations. The x_P dependence is assumed to factorise from the (β, Q^2) dependence and is described by a Regge phenomenological flux factor such that

$$x_P F_2^{D(3)} = A(\beta, Q^2) x_P^{2-2\langle\alpha_P(t)\rangle} \sim x_P^{2-2\langle\alpha_P(t)\rangle}, \quad (2.1)$$

where $\alpha_P(t)$ is the effective pomeron trajectory. The fit describes the data well and results in diffractive parton densities dominated by the gluon density, which extends to large fractional momenta. Similar diffractive parton densities extracted from previous data have been highly successful in describing hadronic final state measurements in diffractive DIS [7].

The hard scattering factorisation proof [6] makes no prediction for the (x_P, t) dependence. From the QCD perspective, the diffractive parton densities could vary in both shape and normalisation with these variables. However, the success of Regge phenomenology in describing soft hadronic cross sections with a universal pomeron trajectory suggests that there may be an extended ‘Regge’ factorisation property whereby the x_P dependence is driven by Regge asymptotics and is completely decoupled from the (β, Q^2) dependence. The dependence on (β, Q^2) then represents a structure function for the exchanged pomeron [8].

In [4], the Regge factorisation hypothesis is tested by measuring the data at a larger number of x_P values² and performing a fit to equation (2.1) with free parameters for the effective pomeron intercept $\alpha_P(0)$ and $A(\beta, Q^2)$ at each (β, Q^2) point. At large x_P (equivalently small γ^*p centre of mass energy W), contributions from sub-leading exchanges are required³ in order to obtain a good fit to the data, although the normalisation and effective intercept of this contribution is not well constrained. The fit yields $\alpha_P(0) = 1.173 \pm 0.018 \text{ (stat.)} \pm 0.017 \text{ (syst.)} \pm_{-0.035}^{+0.063} \text{ (model)}$, the dominant upward model dependence uncertainty arising from the unknown contribution of the cross section for longitudinally polarised photons. The Regge factorisation hypothesis works well within the kinematic range measured in [4], with no significant variation of the effective $\alpha_P(0)$ with β or Q^2 . There is thus no experimental evidence at the present level of precision for a variation of the diffractive parton densities with x_P . The measured $\alpha_P(0)$ is compared with previous

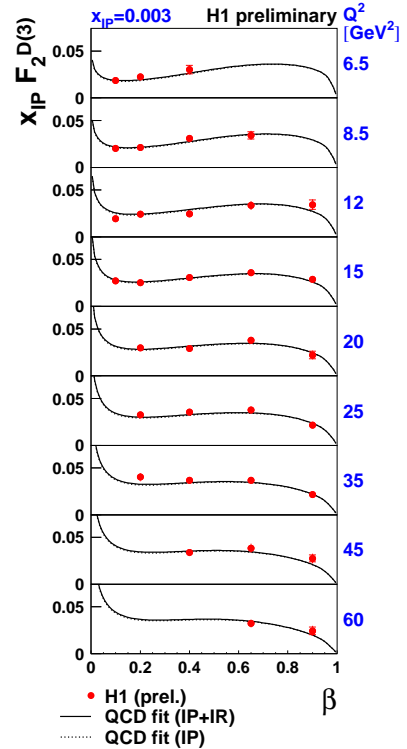


Figure 3: Dependence of $x_P F_2^{D(3)}$ on β for different Q^2 values, with fixed $x_P = 0.003$. The data are compared with the DGLAP QCD fit described in the text (from [4]).

² $F_2^{D(3)}$ is measured at a total of 312 points in the (β, Q^2, x_P) phase space.

³ The fit yields a χ^2 of 0.95 (1.25) per degree of freedom with (without) a sub-leading term included.

DIS and photoproduction measurements and a recent ZEUS measurement in the low Q^2 transition region [9] in figure 4. The result for diffractive DIS is significantly larger than that describing soft hadronic and photoproduction cross sections [10].

Simple Regge predictions for the total γ^*p cross section lead at fixed Q^2 to

$$F_2(x, Q^2) \propto x^{1-\alpha_{\mathbb{P}}(0)}. \quad (2.2)$$

Figure 4 also shows the effective pomeron intercept extracted from inclusive DIS at low x using equation (2.2) [11]. The effective intercepts describing the inclusive and diffractive energy dependences become different at large Q^2 . From equations (2.1) and (2.2), Regge pole models predict a factor of approximately 2 difference in the power of the growth of the diffractive and inclusive cross sections with decreasing x (increasing W). Experimentally, the ratio of diffractive to inclusive cross sections in DIS is found to be relatively flat as a function of x when M_x , β and Q^2 are fixed [2, 4]. The situation for the low Q^2 transition region is rather different [9], since the Regge predictions for the ratio of diffractive to inclusive cross sections work well.

3. Comparisons with Dipole Models

The hard scattering factorisation proof for diffractive DIS does not specify the relationship between the diffractive and the inclusive parton densities. Specific models (e.g. [12, 5]) have been developed for this relationship. A popular approach is to consider the interaction in the proton rest frame, in terms of the elastic and total cross sections for the scattering on the target of $q\bar{q}$ and $q\bar{q}g$ fluctuations of the virtual photon, treated as colour dipoles. Using ideas such as the optical theorem, the same ‘dipole cross section’ can be used to describe total, elastic and dissociative cross sections, thus unifying the description of F_2 and F_2^D . As yet, there is no consensus on the proper way to treat the dipole cross section.

In the ‘saturation’ model [5], the $q\bar{q}$ dipole cross section is obtained from a 3 parameter fit to F_2 data and is then used to predict F_2^D , under the assumption that the diffractive cross section is driven by 2-gluon exchange.⁴ A contribution from $q\bar{q}g$ fluctuations is added in the diffractive case, assumed to interact with the same dipole cross section as the $q\bar{q}$ fluctuation. Figure 5 shows a comparison of the ‘saturation’ model with various diffractive data from ZEUS [2, 9]. The description is good for $Q^2 \geq 4 \text{ GeV}^2$. The $q\bar{q}g$ contribution is clearly needed at large M_x . As yet, the model is not able to describe the low Q^2 region.

Considering the small number of parameters, the model in [5] gives a good description of the new H1 data in [4], though there are clear discrepancies in the small β , small

⁴The prediction is for $F_2^{D(4)}$ at $t = 0$. To describe the $F_2^{D(3)}$ data, an additional free parameter is needed, corresponding to the exponential t dependence, parameterised as e^{Bt} .

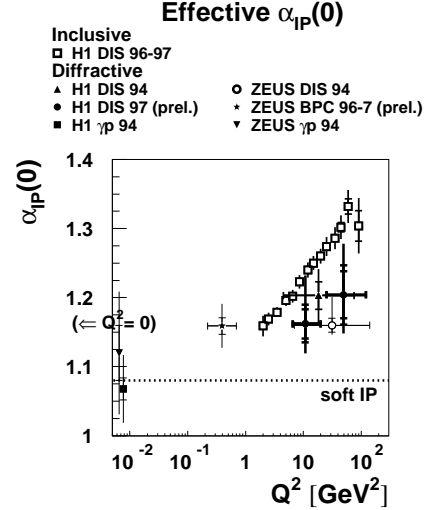


Figure 4: Compilation of values extracted for the effective pomeron intercept in inclusive and diffractive ep scattering, shown as a function of Q^2 .

Q^2 region. Including QCD evolution of the gluon distribution [13] does not improve the description of the data.

In the “semi-classical” model [12], the dipole cross section is modelled as the scattering from a superposition of colour fields of the proton according to a simple non-perturbative model. All resulting final state configurations contribute to the inclusive proton structure function. Those in which the scattered partons emerge in a net colour-singlet state contribute to the diffractive structure function. The model contains only four free parameters, which are obtained from a combined fit to previous F_2 and F_2^D data. The model reproduces the general features of the F_2^D data in [4], but also lies above the data where β and Q^2 are both small.

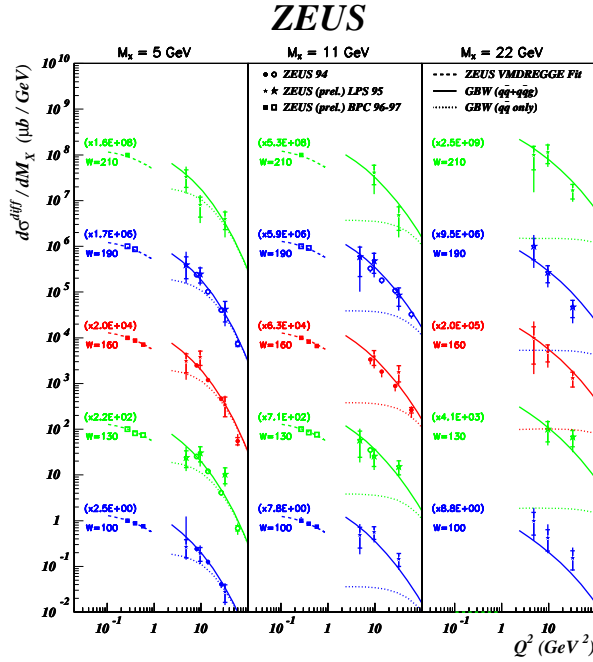


Figure 5: Compilation of ZEUS F_2^D data, compared at high Q^2 with the “saturation” model [5] and at low Q^2 with a Regge motivated parameterisation.

References

- [1] H1 Collaboration, C. Adloff et al., *Z. Physik C* **76** (1997) 613 [hep-ex/9708016].
- [2] ZEUS Collaboration, J. Breitweg et al., *Eur. Phys. J. C* **6** (1999) 43 [hep-ex/9807010].
- [3] F. Goebel, these proceedings.
- [4] H1 Collaboration, abstract 808, paper submitted to EPS Conference on HEP 2001, Budapest.
- [5] K. Golec-Biernat and M. Wüsthoff, *Phys. Rev. D* **60** (1999) 114023 [hep-ph/9903358].
- [6] J. Collins, *Phys. Rev. D* **57** (1998) 3051, Erratum-ibid. **D 61** (2000) 019902 [hep-ph/9709499].
- [7] R. Wichmann, these proceedings.
- [8] G. Ingelman and P. Schlein, *Phys. Lett. B* **152** (1985) 256.
- [9] ZEUS Collaboration, paper 435 submitted to International Conference on HEP 2000, Osaka.
- [10] A. Donnachie and P. Landshoff, *Phys. Lett. B* **296** (1992) 227 [hep-ph/9205235].
- [11] H1 Collaboration, C. Adloff et al., *Phys. Lett. B* **520** (2001) 183 [hep-ex/0108035].
- [12] W. Buchmüller, T. Gehrmann and A. Hebecker, *Nucl. Phys. B* **537** (1999) 477 [hep-ph/9808454].
- [13] K. Golec-Biernat and M. Wüsthoff, *Eur. Phys. J. C* **20** (2001) 313 [hep-ph/0102093].